Thermodynamic stability of La2Mo2–yWyO9 , La2Mo2–yWyO8.96+0.02y and La7Mo7(2–y)/2W7y/2O30 (y = 0, 0.5 and 1.0)

Jesús Vega-Castillo, Uday Ravella, Gwenaël Corbel, Philippe Lacorre, Alberto Caneiro

HAL Id: hal-02131620
https://univ-lemans.hal.science/hal-02131620

Submitted on 17 Jul 2019

Thermodynamic stability of $La_2Mo_{2-y}W_yO_9$, $La_2Mo_{2-y}W_yO_{8.96+0.02y}$ and $La_7Mo_{7(2-y)/2}W_{7y/2}O_{30}$ (y=0, 0.5 and 1.0)$\ddot{A}$

Jesús E. Vega-Castillo[a,b], Uday K. Ravella[c], Gwenaël Corbel[c], Philippe Lacorre[c] and Alberto Caneiro[*a,b,d]

Abstract

The role of W content on the limit oxygen partial pressure (pO_2) for stability of fast oxygen-ion conductors $La_2Mo_{2-y}W_yO_9$ with y = 0, 0.5 and 1.0 has been studied by means of thermogravimetric analysis (TGA) under controlled atmospheres. At 718 °C, below the pO_2 stability limit of $La_2Mo_{2-y}W_yO_9$, the perovskite related compounds $La_7Mo_{7(2-y)/2}W_{7y/2}O_{30}$ were stabilized even for y = 1.0. At 608 °C, the first stage of reduction of β-$La_2Mo_{2-y}W_yO_9$ leads to the formation of the crystallized oxygen deficient $La_2Mo_{2-y}W_yO_{8.6+0.02y}$ phase. X-ray powder diffraction shows that the stabilization of the high temperature β-form through tungsten substitution observed in fully oxidized $La_2Mo_{2-y}W_yO_9$ samples is preserved upon slight reduction. The n-type conductivity arising from the mixed valence state of molybdenum becomes less and less predominant as the W content increases. Further reduction causes amorphization. At both temperatures, W substitution does not enhance the thermodynamic stability of the $La_2Mo_{2-y}W_yO_9$ ion conductor under a reducing atmosphere but only slows down the kinetics of reduction.

Introduction

$La_2Mo_2O_9$ is a fast oxide-ion conductor whose conductivity is higher than that reported for Yttria Stabilized Zirconia (8 mol% YSZ), the currently used electrolyte material for solid oxide fuel cells (SOFC).[1] The use of an electrolyte with higher conductivity than YSZ is a way to decrease both the operating temperature and cost of SOFCs, since expensive interconnection materials would not be needed for their fabrication.[2] $La_2Mo_2O_9$ undergoes an order–disorder transition from a monoclinic α to a cubic β form with an increase of the conductivity by almost 2 orders of magnitude.[3] LAMOX is the common name for the family of ionic conductors based on isovalent and aliovalent substitutions in $La_2Mo_2O_9$.[4–17] Several cationic substitutions in LAMOX compounds stabilize the highly conducting beta phase down to room temperature.

The main drawback of implementing $La_2Mo_2O_9$ as an electrolyte for Intermediate Temperature SOFCs (IT-SOFC) is its poor stability under reducing atmospheres. Several authors have reported the decomposition of $La_2Mo_2O_9$ at temperatures above 600 °C in dilute H_2.[18–21] The W substituted LAMOX compounds $La_2Mo_{2-y}W_yO_9$ have been reported to show better stability against reduction than the parent compound $La_2Mo_2O_9$. Georges et al. analyzed oxygen loss as a function of W content in $La_2Mo_{2-y}W_yO_9$ powders after being annealed at 605 °C in dilute H_2 (6% H_2–94% N_2) for 16 h.[18] They found that the weight loss is lower when the W content increases and it is even null for y = 1.4. Marrero-López et al. determined the limit oxygen partial pressure (pO_2) of $La_2Mo_{2-y}W_yO_9$ samples as a function of x by Coulometric titration.[19] The authors claimed that the limit values of pO_2 for stability of the LAMOX structure are lower for W substituted compounds, at a given temperature. This would mean that doping with W on LAMOX might help overcome the serious drawback of instability under reducing atmospheres, in order to consider these materials as electrolytes for IT-SOFCs. The substitution of Mo by W causes the retention of the β cubic phase for y > 0.1 at room temperature and decreases slightly the ionic conductivity of these compounds.

In our previous work we studied the stability of $La_2Mo_2O_9$ under reducing atmospheres by Thermogravimetric Analysis (TGA) using an electrochemical system for controlling pO_2.[22] In the mentioned work, we determined the limit pO_2 for

[a]Instituto Balseiro, Centro Atómico Bariloche, 8400 San Carlos de Bariloche, Río Negro, Argentina. E-mail: caneiro@cab.cnea.gov.ar
[b]Consejo Nacional de Investigaciones Científicas y Técnicas CONICET, Argentina
[c]LUNAM Université, Université du Maine, CNRS UMR 6283, Institut des Molécules et Matériaux du Mans, Avenue Olivier Messiaen, 72085 Le Mans Cedex 9, France
[d]Comisión Nacional de Energía Atómica CNEA, Argentina
† CCDC reference numbers 955399 and 955400.

stability of $La_2Mo_2O_9$ and found stabilization of $La_7Mo_7O_{30}$ at 718 °C and of the mixed ionic and electronic conductor (MIEC) $La_2Mo_2O_{8.96}$ at 608 °C. In the present work, we have extended this analysis to $La_2Mo_{2-y}W_yO_9$ samples with $y = 0.5$ and 1.0. This study was restricted to compositions having a tungsten content lower than $y = 1.2$ because at higher substitution rate, the high temperature beta form is not thermodynamically stable in air above 700 °C.[23] In this way we obtained a new insight into the effect of W on the thermodynamic stability of LAMOX materials and the stabilization of other compounds, as products of their partial reduction.

Experimental

$La_2Mo_{2-y}W_yO_9$ powders were synthesized by a solid state reaction method. Stoichiometric amounts of La_2O_3, MoO_3 and WO_3 were ground manually in an agate mortar. La_2O_3 was previously dehydrated and decarbonated at 1000 °C for 1 h. The mixture was first annealed in air at 500 °C for 12 h and then at 900 °C ($y = 0$), 1025 °C ($y = 0.5$) and 1075 °C ($y = 1.0$) for another 12 h. Several intermediate grinding and heat treatments were necessary in order to obtain single phases.

Dense $La_2Mo_{2-y}W_yO_9$ pellets were made from as prepared powders. The raw powders were previously ball-milled in a RETSCH planetary mill apparatus with 20 agate balls (1 cm diameter) for 15 min at 580 rpm, in order to decrease the particles size. Then, the milled powders were shaped into a cylindrical form (~5 mm diameter and thickness) by pressing uniaxially under 1 ton. The green pellets were fired at 1200 °C for 2 h. The sintered pellets gave relative densities above 90%.

TGA measurements of the oxygen content of $La_2Mo_{2-y}W_yO_{9-\delta}$ as a function of pO_2 were carried out in a Cahn 1000 thermobalance coupled to an electrochemical gas control system. The whole equipment has been described elsewhere.[24] The experiments were performed on ~500 mg of the starting La_2Mo_{2-y}-W_yO_9 raw powders. The sample was heated up to the working temperature in Ar. After reaching the equilibrium of the TGA signal, the mass in dry air was used as a reference for stoichiometric values ($9 - \delta = 9$). The equilibrium at a set pO_2 was assumed once the TGA signal presented a variation of less than 10 µg for at least 5 h. The pO_2 was then decreased until equilibrium was reached again. Different gas mixtures (Ar for the highest pO_2 values, CO–CO_2 for intermediate values and Ar–H_2–H_2O for low pO_2) were used to scan a wide pO_2 range. The experimental conditions were the same as those described in our previous work.[22]

The phase purity of powders and pellets samples was checked by X-ray diffraction (XRD) by means of a Philips PW1700 diffractometer with a graphite monochromator ($Cu(K_{\alpha 1} + K_{\alpha 2})$ radiation) and of a PANalytical θ/θ Bragg-Brentano X'pert MPD PRO diffractometer ($Cu(K_{\alpha 1} + K_{\alpha 2})$) with an X'Celerator multi-element detector. XRD patterns of $La_7Mo_{7(2-y)/2}W_{7y/2}O_{30}$ with $y = 0$, 0.5 and 1.0 were refined by Rietveld's method with the Fullprof Suite package.[25] The diffractograms were collected in the scattering range $9 < 2\theta < 130°$ with a step of 0.008° and a counting time of 100 s per step.

Isothermal XRD measurements at controlled temperature (HTXRD) in controlled pO_2 were performed in an Anton-Paar HTK10 camera connected to the electrochemical control system mentioned above.

$La_2Mo_{2-y}W_yO_{9-\delta}$ samples, with $y = 0$, 0.5 and 1.0, were characterized electrically by electrochemical impedance spectroscopy (EIS) with an Autolab potentiostat and a frequency response analyzer (FRA). Prior to measurements, thin Pt film electrodes of approximately 400 nm thickness were deposited by RF sputtering on both flat faces of each sintered pellet. The pellet sample was first heated in air up to 608 °C. Then the air atmosphere was replaced with Ar–H_2–H_2O atmosphere and EIS spectra were recorded as a function of time at 608 °C for ≈42 h and then at decreasing temperature. EIS spectra were collected in the frequency range from 1 MHz down to 100 mHz with a voltage amplitude of 50 mV. The obtained spectra were fitted using equivalent circuits of Zview software.[26]

Results and discussion

Oxygen content in $La_2Mo_{2-y}W_yO_{9-\delta}$ as a function of pO_2 at 718 °C

Fig. 1 shows the equilibrium oxygen content $9 - \delta$ as a function of pO_2 of powder samples of $La_2Mo_{2-y}W_yO_{9-\delta}$ at 718 °C. All three compositions exhibit the same limit pO_2 value for stability of the β-$La_2Mo_2O_9$-type structure (oxygen content equal to 9): 10^{-15} atm. This is a surprising result since it was expected that with increasing the W content, the pO_2 limit value becomes lower, thus indicating the broadening of the stability range. The only difference noticed for the three samples while decreasing pO_2 from 10^{-15} down to 10^{-16} atm was the elapsed time before reaching equilibrium of the TGA signal at an oxygen content of 8.57. This reduction stage took 5, 8 and 10 days for $y = 0$, 0.5 and 1.0, respectively. These
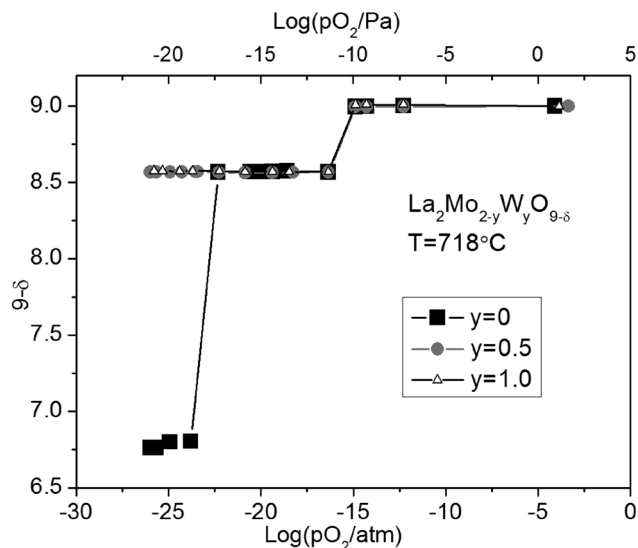

Fig. 1 Oxygen content as a function of pO_2 in $La_2Mo_{2-y}W_yO_{9-\delta}$ powders at 718 °C.

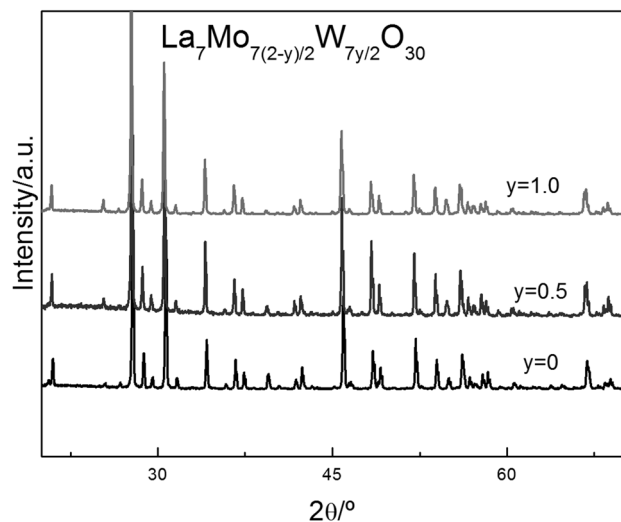**Fig. 2** XRD patterns at room temperature of $La_2Mo_{2−y}W_yO_{8.57}$ samples.

Fig. 3 Observed (dots), calculated (lines), and difference (below) patterns of $La_7Mo_{7(2−y)/2}W_{7y/2}O_{30}$: (a) y = 0.5; (b) y = 1.0 at room temperature using the structural model presented in Table 1. Vertical markers give Bragg peak positions of space group $R\bar{3}$ (no. 148).

results indicate that W does not modify the thermodynamic stability of $La_2Mo_{2−y}W_yO_9$ compounds, but its effect would be to slow down the kinetics of reduction.

After stabilizing the oxygen content at 8.57 in each of the three experiments, the pO_2 was decreased gradually down to $10^{−27}$ atm, with a minimum dwelling time of 5 h at each pO_2 value. The two W doped samples did not undergo any further reduction unlike that observed for y = 0.[22] The oxygen content for y = 0.5 and 1.0 samples remained 8.57 even upon switching the atmosphere to dry Ar–H$_2$ (the atmosphere in which the pO_2 is immeasurably low). This indicates that W does stabilize at 718 °C the compounds with a stoichiometry of 8.57, avoiding their further reduction.

The samples $La_2Mo_{2−y}W_yO_{8.57}$ with y = 0.5 and 1.0 were quenched down to room temperature in Ar–H$_2$ for XRD analysis. In Fig. 2 the obtained diffractograms are compared to those obtained previously for $La_7Mo_7O_{30}$.[22] The W doped stabilized compounds are clearly isomorphic to $La_7Mo_7O_{30}$ and have the formula $La_7Mo_{7(2−y)/2}W_{7y/2}O_{30}$. Marrero-López et al. reported the formation of this kind of compound upon partial reduction of $La_2Mo_{2−y}W_yO_9$ powders but only for y up to 0.75.[19] To the best of our knowledge the crystalline structures of $La_7Mo_{7(2−y)/2}W_{7y/2}O_{30}$ compounds have not been reported to date.

Crystalline structure of $La_7Mo_{7(2−y)/2}W_{7y/2}O_{30}$ (y = 0.5 and 1.0)

The structure of $La_7Mo_{7(2−y)/2}W_{7y/2}O_{30}$ compounds with y = 0.5 and 1.0 was refined by adjusting XRD patterns by Rietveld's method. The crystallographic data of $La_7Mo_7O_{30}$ (ICSD #50614) were used as the starting structural model for refinement. The patterns were adjusted in the $R\bar{3}$ space group (no. 148). The refined crystallographic parameters were: lattice parameters, atomic positions and isotropic displacement factors.

The refinements of diffractograms of $La_7Mo_{7(2−y)/2}W_{7y/2}O_{30}$ with y = 0.5 and 1.0 are shown in Fig. 3(a) and (b), respectively. The list of crystallographic parameters and reliability factors
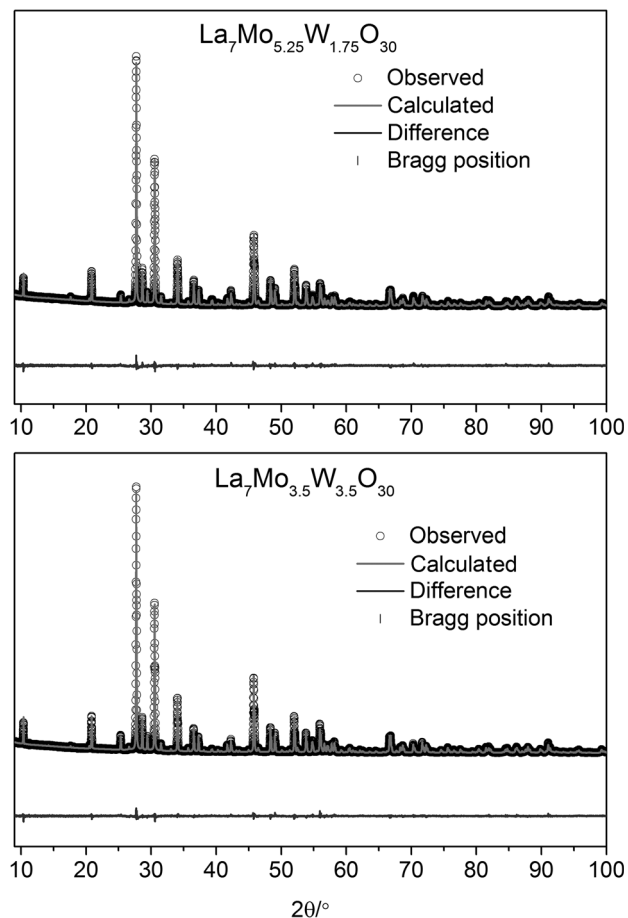
obtained from the refinements is presented in Table 1. The relatively large profile weighted factors (Rwp) are likely due to the low signal/background ratio of both refined diffractograms.

The lattice parameters a and c, compared to those of $La_7Mo_7O_{30}$, increase with W content as shown in Fig. 4. The structure has two crystallographic sites for La, one in coordination 12 and the other in coordination 9; there are also two sites for Mo|W, both in coordination 6.[20] The (Mo|W)1O$_6$ octahedra are regular whereas (Mo|W)2O$_6$ are distorted.

Oxygen content in $La_2Mo_{2−y}W_yO_{9−δ}$ as a function of pO_2 at 608 °C

Fig. 5 shows the oxygen content of $La_2Mo_{2−y}W_yO_9$ powders with y = 0, 0.5 and 1.0 as a function of pO_2 at 608 °C. All three LAMOX samples present the same pO_2 limit value of $10^{−22}$ atm for stoichiometry 9 regardless of the W amount. After decreasing pO_2 down to $10^{−23}$ atm, a slight reduction occurs to oxygen contents 8.97 and 8.98 for W doped samples with y = 0.5 and 1.0, respectively. At this temperature, the time needed to reach the equilibrium increases with the W amount thus indicating that once again, W slows down the reduction kinetics. The

Table 1 Lattice constants, reliability factors and crystallographic parameters obtained from Rietveld's refinement of $La_7Mo_{5.25}W_{1.75}O_{30}$ and $La_7Mo_{3.5}W_{3.5}O_{30}$ (in cursive)

a/Å	c/Å	R_{wp}/%	R_{exp}/%	R_{Bragg}/%	χ^2
17.0164(1)	6.8716(1)	13.2	9.77	6.44	1.819
17.022(1)	*6.8759(1)*	*12.3*	*8.67*	*5.87*	*2.025*

Atom	Wyckoff	x/a	y/b	z/c	U_{iso}/Å^2
La1	3a	0	0	0	0.0080(2)
		0	*0*	*0*	*0.0072(2)*
(Mo|W)1	3b	0	0	0.5	0.0019(2)
		0	*0*	*0.5*	*0.00307(2)*
La2	18f	0.7780(1)	−0.0177(1)	0.3345(3)	0.0080(2)
		0.7760(1)	*−0.0189(1)*	*0.3368(3)*	*0.0072(2)*
(Mo|W)2	18f	0.1997(1)	0.0146(1)	0.1629(3)	0.0019(2)
		0.1997(1)	*0.0159(1)*	*0.1636(3)*	*0.0031(2)*
O1	18f	0.2478(1)	0.1007(7)	0.3584(2)	0.001(1)
		0.2510(8)	*0.0100(1)*	*0.3661(2)*	*0.0016(1)*
O2	18f	0.2918(8)	0.0373(8)	0.0084(2)	0.001(1)
		0.2902(7)	*0.0363(7)*	*−0.0215(2)*	*0.0016(1)*
O3	18f	0.1796(6)	0.1230(6)	0.0427(2)	0.001(1)
		0.1796(6)	*0.1236(6)*	*0.0411(2)*	*0.0016(1)*
O4	18f	0.2032(7)	−0.0848(7)	0.3197(1)	0.001(1)
		0.2029(7)	*−0.0764(7)*	*0.3179(1)*	*0.0016(1)*
O5	18f	0.0396(6)	0.1082(6)	0.3297(2)	0.001(1)
		0.0355(6)	*0.1043(5)*	*0.3292(16)*	*0.0016(1)*

Fig. 4 Lattice parameters of $La_7Mo_{7(2-y)/2}W_{7y/2}O_{30}$ as a function of W content.

Fig. 5 Oxygen content as a function of pO_2 in $La_2Mo_{2-y}W_yO_{9-\delta}$ powders at 608 °C.

oxygen content remains practically invariant down to 10^{-26} atm. The compounds $La_2Mo_{1.5}W_{0.5}O_{8.97}$ and $La_2MoWO_{8.98}$ have a pO_2 stability range which is slightly wider than that of $La_2Mo_2O_{8.96}$.[22] It shows that W substitution enhances very slightly the stability under reducing atmospheres of the $La_2Mo_2O_{8.96}$-type phase.

Below this pO_2, a severe reduction takes place in all three compounds and ends with oxygen contents lower than 7.0, 7.5 and 8.0 for $y = 0$, 0.5 and 1.0 respectively. These points were not strictly equilibrated and as previously described for $y = 0$,[22] they exhibit a linear drift. At this point, all samples were quenched down to room temperature and post-analyzed by XRD. The results of XRD analysis on the three severely reduced samples is shown in Fig. 6. For $y = 0$ the diffractogram exhibits undulations of the background without any Bragg reflections, indicating that the sample is amorphous in nature. For $y = 0.5$
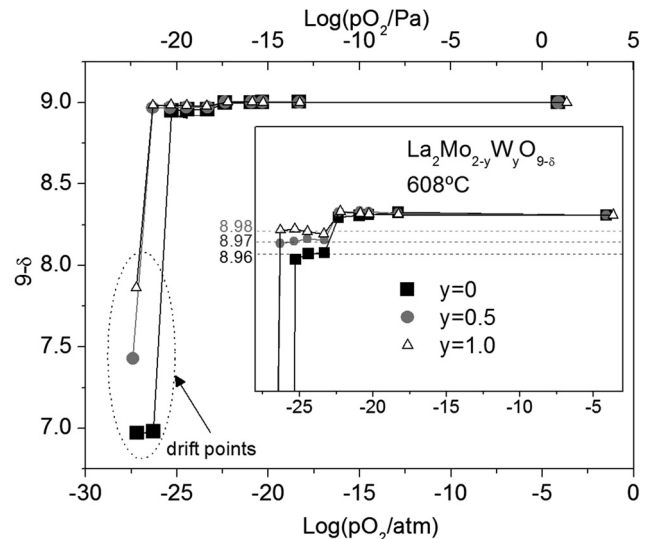
and $y = 0.1$ samples, several diffraction peaks ascribed to a β-$La_2Mo_2O_9$-type phase are present in addition to the amorphous phase. These peaks grow in intensity as the W amount increases. The higher the W content of the sample, the higher the average oxygen content and the amount of the remaining crystallized β-$La_2Mo_2O_9$-type phase.

In order to collect XRD patterns on $La_2Mo_{1.5}W_{0.5}O_{8.97}$ and $La_2MoWO_{8.98}$ compounds, approximately 500 mg of $La_2Mo_{1.5}W_{0.5}O_9$ and La_2MoWO_9 raw powders were annealed inside the thermobalance at 608 °C under atmospheres with a set pO_2 of 10^{-24} atm. The TGA signal reached the steady state at oxygen contents of 8.97 and 8.98 after 280 and 320 min,
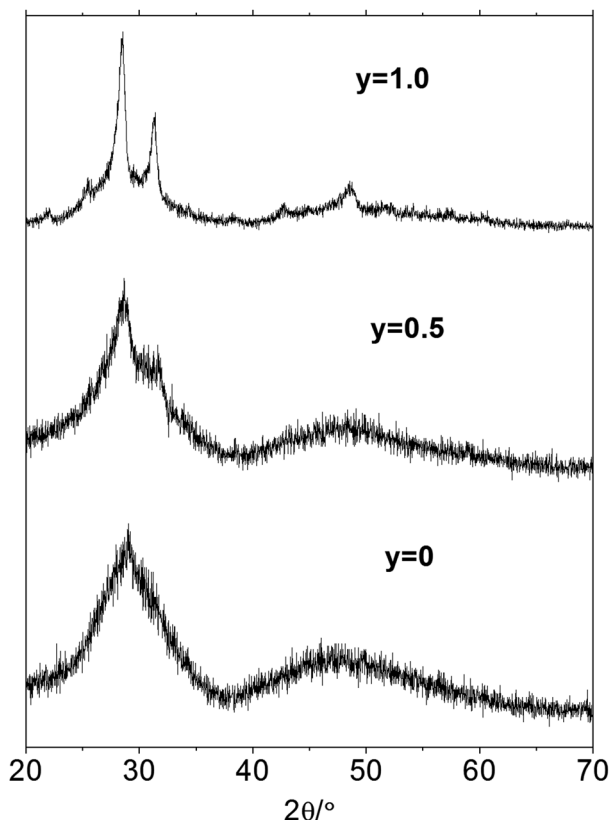
Fig. 6 XRD patterns of quenched severely reduced samples of $La_2Mo_{2-y}W_yO_{9-\delta}$ with y = 0, 0.5 and 1.0.

Fig. 7 XRD diagrams of $La_2Mo_{1.5}W_{0.5}O_{8.97}$ and $La_2MoWO_{8.98}$ powders at room temperature: (a) extended range; (b) zoom around cubic reflection (2 3 1).

respectively. At this point the samples were quenched down to room temperature while keeping the controlled atmosphere. The resulting powders presented a bronze color very similar for both W-substituted samples but different from the light gray of previously stabilized $La_2Mo_2O_{8.96}$ powders.[22]

In Fig. 7, the XRD patterns collected at room temperature on $La_2Mo_{1.5}W_{0.5}O_{8.97}$ and $La_2MoWO_{8.98}$ powders exhibit neither $2 \times 3 \times 4$ superstructure peaks at low 2θ scattering angle nor peak splitting, both characteristic of the monoclinic distortion of the low temperature β-$La_2Mo_2O_9$ type. This indicates that the stabilization of the high temperature β form through tungsten substitution is preserved in spite of the slight reduction. When compared with XRD patterns of fully oxidized $La_2Mo_{1.5}W_{0.5}O_9$ and La_2MoWO_9 samples, the diffraction peaks of the reduced phases are slightly shifted in position toward higher 2θ angles, thus involving a contraction of the unit cell after reduction. The cubic cell parameters obtained from Rietveld's refinement at room temperature in the $P2_13$ space group are 7.1559(1) and 7.1528(1) Å for $La_2Mo_{1.5}W_{0.5}O_{8.97}$ and $La_2MoWO_{8.98}$ compared to 7.1598(1) and 7.1534(1) Å of the original $La_2Mo_{1.5}W_{0.5}O_9$ and La_2MoWO_9. This behavior had been previously observed upon reducing $La_2Mo_2O_9$ into $La_2Mo_2O_{8.96}$.[22]

If one assumes that only hexavalent molybdenum is reduced, the ionic charge balance for the chemical formulas $La_2Mo_2O_{8.96}$, $La_2Mo_{1.5}W_{0.5}O_{8.97}$ and $La_2MoWO_{8.98}$ yields a

valence value of 5.96+ for Mo for all three cases. Marrero-López *et al.* performed X-ray photoelectron spectroscopy (XPS) on reduced $La_2Mo_{2-y}W_yO_{9-\delta}$ and confirmed that only Mo had been reduced.[27] Therefore, a general chemical formula for this group of compounds would be $La_2Mo_{2-y}W_yO_{8.96+0.02y}$.

The contraction of crystal cells of $La_2Mo_{2-y}W_yO_{8.96+0.02y}$ with respect to the corresponding original $La_2Mo_{2-y}W_yO_9$ materials was studied by HTXRD. $La_2Mo_{2-y}W_yO_9$ powders with y = 0, 0.5 and 1.0 were heated up to 608 °C in He and then the atmosphere was switched by He–Ar–H$_2$–H$_2$O with a set pO_2 of 10^{-24} atm. After annealing for 2 h, the stabilization of $La_2Mo_2O_{8.96}$, $La_2Mo_{1.5}W_{0.5}O_{8.97}$ and $La_2MoWO_{8.98}$ respectively was assumed. All diffractograms were refined by Rietveld's method in the $P2_13$ space group. It is worth mentioning that above 560 °C both $La_2Mo_2O_9$ and $La_2Mo_2O_{8.96}$ are in cubic beta form.[22] Fig. 8(a) shows the cell parameters of cubic samples of $La_2Mo_{2-y}W_yO_9$ (black line) and $La_2Mo_{2-y}W_yO_{8.96+0.02y}$ (gray line) with y = 0, 0.5 and 1.0 at 608 °C as a function of y. The dependence in both groups of compounds is different. For example, the cell parameter of $La_2Mo_{1.5}W_{0.5}O_9$ is slightly larger than that of La_2MoWO_9, whereas the cell parameter of $La_2Mo_{1.5}W_{0.5}O_{8.97}$ is smaller than that of

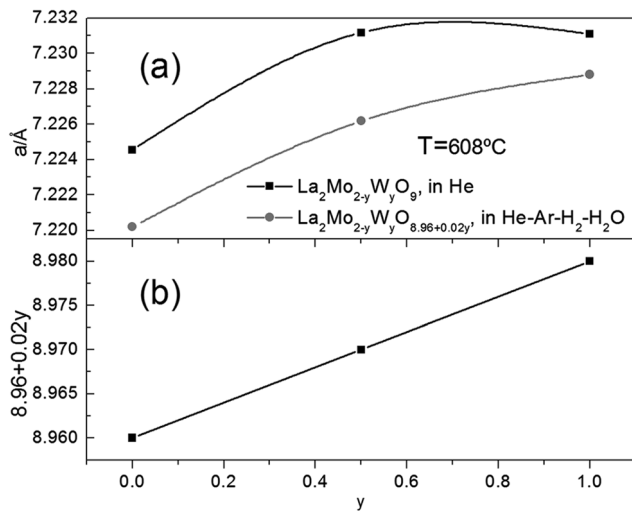**Fig. 8** (a) Cell parameters of $La_2Mo_{2-y}W_yO_9$ and $La_2Mo_{2-y}W_yO_{8.96+0.02y}$ calculated from HTXRD patterns at 608 °C; (b) oxygen content of $La_2Mo_{2-v}W_yO_{8.96+0.02y}$ as a function of W content.

Fig. 10 EIS spectra measured at 450 °C on dense pellet samples of $La_2Mo_{2-y}W_yO_9$ in air and $La_2Mo_{2-y}W_yO_{8.96+0.02y}$ measured in $Ar-H_2-H_2O$, with: (a) y = 0; (b) y = 0.5; (c) y = 1.0.

$La_2MoWO_{8.98}$. The cell parameters of $La_2Mo_{2-y}W_yO_{8.96+0.02y}$ depend not only on the W content but also on the oxygen stoichiometry which in turn depends linearly on y, as noticed in Fig. 8(b). The gray curve in Fig. 8(a) seems to be a behavior that combines the black line in Fig. 8(a) and the curve in Fig. 8(b).

Electrical characterization of dense $La_2Mo_{2-y}W_yO_{8.96+0.02y}$ samples

The total resistance of $La_2Mo_{2-y}W_yO_{9-\delta}$ (with y = 0, 0.5 and 1.0) pellet samples at 608 °C was measured as a function of time by EIS in an $Ar-H_2-H_2O$ mixture with a set pO_2 of 10^{-24} atm. The time evolution of the resistance values R for the three pellet samples is shown in Fig. 9; the initial value corresponds to the fully oxidized $La_2Mo_{2-y}W_yO_9$ pellet sample measured in air. After 2500 s the three R values stabilized and this was
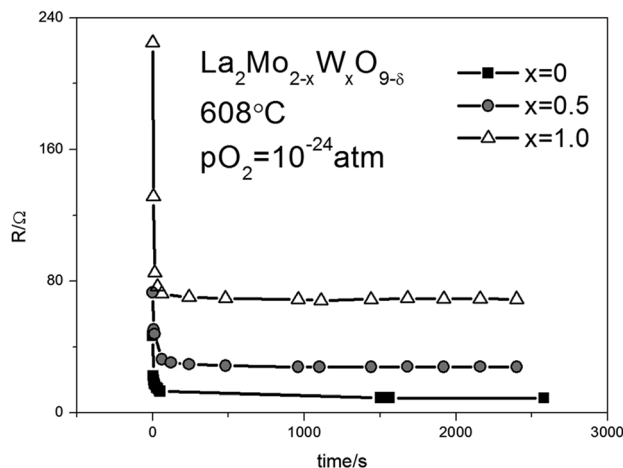

Fig. 9 Bulk resistance of $La_2Mo_{2-y}W_yO_{9-\delta}$ ceramics obtained from EIS spectra.

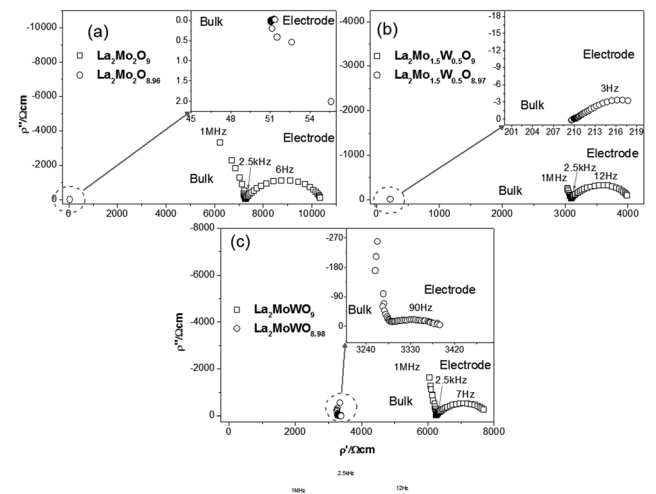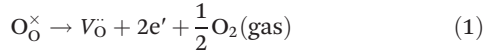assumed to be indicative of the stabilization of $La_2Mo_{2-y}W_yO_{8.96+0.02y}$ compounds. At this point EIS spectra were collected at different temperatures while cooling down to 250 °C under the same atmosphere.

Fig. 10 shows the comparison of EIS spectra of $La_2Mo_{2-y}W_yO_9$ and $La_2Mo_{2-y}W_yO_{8.96+0.02y}$ measured at 450 °C for (a) y = 0, (b) y = 0.5 and (c) y = 1.0. For each composition the reduction of oxygen content from 9 to 8.96 + 0.02y leads to a decrease of polarization resistance (distances between the origin and the first intercept with the real axis). This decrease is less important as the W content increases. Another consequence of the reduction for y = 0 and 0.5 samples is that the high frequency range of the spectra, corresponding to the bulk, is no longer a semicircle with a negative imaginary part (capacitive reactance) but the spectra start at positive imaginary values (inductive reactance) before intercepting the real axis. The suppression of the capacitive effect could be assigned to the apparition of electronic conductivity across the bulk. The capacitive effect, in an electrochemical cell with a pure ion conductor bulk, is caused by the accumulation of electrical charge at the electrode/electrolyte interfaces because the mobility of O^{2-} ions is much lower than that of electrons. In other words, the current of the circuit delays (negative phase difference) with respect to the external voltage signal. If the bulk has electronic conductivity, the capacitive effect disappears and the phase difference of the current could be positive due to the inductive effect of the electrical contacts. A similar behavior has been observed by Pinet *et al.* studying the electrical properties of $La_{1.9}Y_{0.1}Mo_{2-y}W_yO_{9-\delta}$ under dilute H_2 by EIS.[28]

As shown in Fig. 10(c), for y = 1.0, the decrease of resistivity after reduction is only around 50% and the spectrum of $La_2MoWO_{8.98}$ still shows the last portion of a semicircle similar to that of La_2MoWO_9. These results suggest that the partial reduction of $La_2Mo_{2-y}W_yO_9$ to $La_2Mo_{2-y}W_yO_{8.96+0.02y}$ promotes the apparition of electronic conductivity while keeping the ionic conductivity of the stoichiometric

LAMOX compound. In other words, $La_2Mo_{2-y}W_yO_{8.96+0.02y}$ are MIEC.

The apparition of electronic conductivity would be due to the generation of O vacancies upon reduction of Mo; the electric charge would be compensated for by the generation of n-type charge carriers:

$$O_O^\times \rightarrow V_O^{\cdot\cdot} + 2e' + \frac{1}{2}O_2(gas) \tag{1}$$

If all O vacancies are generated by partial reduction, there is a relation between the concentration of electrons $[e']$ and the concentration of O vacancies $[V_O^{\cdot\cdot}]$:

$$2[V_O^{\cdot\cdot}] = [e'] \tag{2}$$

In turn, the concentration of vacancies is proportional to the deviation of stoichiometry δ in $La_2Mo_{2-y}W_yO_{9-\delta}$. In the case of $La_2Mo_{2-y}W_yO_{8.96+0.02y}$, $\delta = 0.04 - 0.02y$. The generated electronic conductivity σ_e would be proportional to the concentration of electrons:

$$\sigma_e = \mu_e[e']e \tag{3}$$

where μ_e is the mobility of electrons and e is their charge.

In this way, the electronic part of total conductivity for $La_2Mo_{2-y}W_yO_{8.96+0.02y}$ would depend on the W content as follows:

$$\sigma_e \propto (2 - y) \tag{4}$$

This would explain why the increase upon reduction from $La_2Mo_{2-y}W_yO_9$ to $La_2Mo_{2-y}W_yO_{8.96+0.02y}$ is larger as the W content decreases. It would also justify the fact that the EIS spectrum of the $La_2MoWO_{8.98}$ sample still shows a semicircle at the bulk zone. The electronic conductivity generated in this MIEC would be low (due to the low δ value of 0.02) and the total conductivity would be mainly ionic.

The EIS spectra of pure ionic conductors $La_2Mo_{2-y}W_yO_9$ and the MIEC $La_2MoWO_{8.98}$ were adjusted with a resistance R in parallel with a constant phase element (CPE). In the case of $La_2Mo_{2-y}W_yO_{8.96+0.02y}$ with $y = 0$ and 0.5, the bulk zone was fitted with a resistance R in series with an inductance L. In all cases, R values were used for calculating the total conductivity of the bulk as

$$\sigma = \frac{L}{RA} \tag{5}$$

where L and A are the thickness and the transversal section area of the dense samples, respectively. For all spectra, the low frequency zone corresponding to the electrode was fitted with a Warburg element.

Fig. 11 shows the Arrhenius plots of conductivity measured for $La_2Mo_{2-y}W_yO_9$ in air (closed symbols) and for $La_2Mo_{2-y}W_yO_{8.96+0.02y}$ in Ar–H$_2$–H$_2$O (open symbols), with $y = 0$, 0.5 and 1.0.

When compared with the conductivity curve of the fully oxidized sample $La_2Mo_2O_9$ below 550 °C, a huge increase of total conductivity and a decrease of the activation energy are observed for $La_2Mo_2O_{8.96}$.[22] The lower the temperature, the
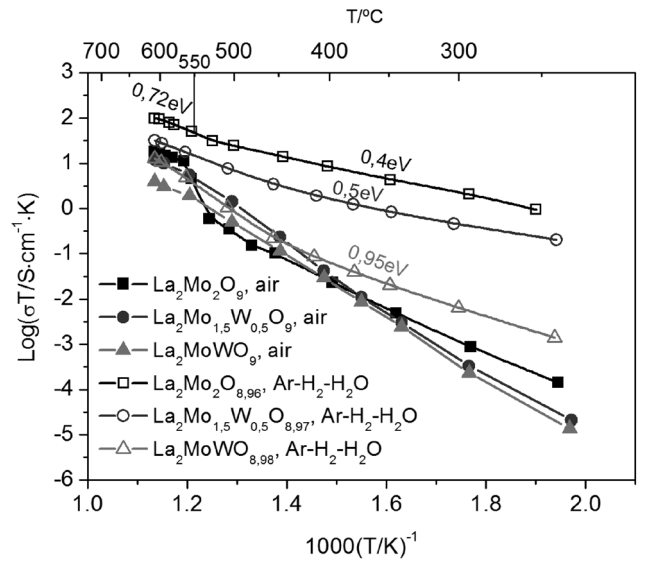

Fig. 11 Conductivity as a function of temperature for the ceramics $La_2Mo_{2-y}W_yO_9$ in air and $La_2Mo_{2-y}W_yO_{8.96+0.02y}$ in Ar–H$_2$–H$_2$O with $y = 0$, 0.5 and 1.0.

higher the magnitude of the increase in conductivity. The difference of several orders of magnitude in conductivity was ascribed to the occurrence of an n-type conductivity arising from the mixed valence state of molybdenum. In the W-substituted sample, the increase in conductivity remains of the same order of magnitude at temperatures higher than 550 °C whatever the W content. This increase exhibits a dependence on tungsten content at lower temperature: the higher the tungsten content, the more pronounced is the effect at low temperature. It suggests that at low temperature, the n-type conductivity becomes less and less predominant as the W content increases. This tendency is somewhat surprising since the proportion of pentavalent molybdenum (or the oxygen content) in reduced samples does not change as much as the total conductivity does.

Jacquens et al. reduced partially $La_2Mo_{2-y}W_yO_9$ dense samples in dry Ar–(10%)H$_2$ at 608 °C and measured their conductivity.[29] The results obtained by the mentioned authors are identical to those reported herein for $y = 0$, 0.5 and 1.0. Similar to our previous work,[22] we conclude that Jacquens and co-authors stabilized $La_2Mo_{2-y}W_yO_{8.96+0.02y}$ in low flow (0.6 L h^{-1}) of Ar–H$_2$. Goel et al. obtained similar conductivity increases at reducing W doped LAMOX samples in dry Ar–(10%)H$_2$ at 650 °C for 24 h, with a gas flow rate of 6 L h^{-1}.[30] For highly dense samples, the oxygen stoichiometries measured after annealing were 7.93, 8.62 and 8.9 for $y = 0$, 0.5 and 1.0, respectively. We think that these authors could have reduced transitorily $La_2Mo_{2-y}W_yO_9$ to $La_2Mo_{2-y}W_yO_{8.96+0.02y}$ but the reduction continued to yield a more severe weight loss and perhaps a partial amorphization of samples. In fact, Goel et al. report a severe degradation of the pellets after reduction. In our case, the mechanical integrity of all $La_2Mo_{2-y}W_yO_{8.96+0.02y}$ pellets after our EIS measurements was perfectly preserved.

Conclusions

Isothermal thermogravimetric and XRD analyses under a controlled pO_2 atmosphere were carried out on $La_2Mo_{1.5}W_{0.5}O_9$ and La_2MoWO_9 phases in order to determine their thermodynamic stability. Contrary to what has been reported earlier in the literature, tungsten substitution does not extend to lower pO_2 values the thermodynamic stability of $La_2Mo_2O_9$ either at 608 °C (10^{-22} atm) or at 718 °C (10^{-15} atm). At both temperatures, tungsten only slows down the kinetics of reduction.

The mechanism by which $La_2Mo_{2-y}W_yO_9$ get reduced regardless of the hexavalent W content is not clear. Such a mechanism should be more sensitive to the structural arrangement and the oxidation state than to the chemical stoichiometry.

After decreasing pO_2 down to 10^{-23} atm, a new crystalline $La_2Mo_2O_{8.96}$-type phase, isostructural to $La_2Mo_2O_9$, appears at 608 °C and remains stable in a pressure range which slightly widens as the W content increases. The stabilization of the high temperature β-form through tungsten substitution observed in fully oxidized $La_2Mo_{2-y}W_yO_9$ samples is preserved upon slight reduction. The electrical conductivity measurements of $La_2Mo_{2-y}W_yO_{8.96+0.02y}$ phases suggest that at temperatures lower than 550 °C, the n-type conductivity arising from the mixed valence state of Mo cations becomes less and less predominant as the W content increases.

The poor stability under reducing atmospheres of W-LAMOX compounds, even at temperatures around 600 °C, limits seriously their applicability as electrolytes in IT-SOFC, at least in the conventional configuration. Of course in such devices with less stringent reduction conditions as single-chamber SOFC, these electrolytes could be stable.[29]

At 718 °C, the stable phase below 10^{-15} atm is more reduced and of the $La_7Mo_7O_{30}$ type ($La_2Mo_2O_{8.57}$). Tungsten extends down to 10^{-27} atm the thermodynamic stability range of this type of phase whereas pure $La_7Mo_7O_{30}$ reduces slowly below 10^{-25} atm down to an amorphous $La_2Mo_2O_{7-\delta}$ phase. The crystal structures of $La_7Mo_{5.25}W_{1.75}O_{30}$ and $La_7Mo_{3.5}W_{3.5}O_{30}$ have been refined from X-ray diffraction data by Rietveld's method.

The partially reduced compounds $La_2Mo_{2-y}W_yO_{8.96+0.02y}$ were found within an intermediate and narrow pO_2 range at 608 °C. These materials keep the LAMOX cationic framework as evidenced by XRD. This fact suggests that these materials preserve the ionic conductivity of $La_2Mo_{2-y}W_yO_9$. The electrical conductivity of $La_2Mo_{2-y}W_yO_{8.96+0.02y}$ was measured by EIS. These partially reduced stable materials showed an increase of conductivity with respect to the stoichiometric $La_2Mo_{2-y}W_yO_9$ electrolytes. The increase of conductivity was assigned to the generation of O vacancies in these materials upon reduction of Mo^{6+} to $Mo^{5.96+}$, whose electrical charge is compensated for by the apparition of n-type carriers.

$La_2Mo_{2-y}W_yO_{8.96+0.02y}$ do not have high electronic conductivity for being considered as potential anode materials for IT-SOFCs. Some authors have reported a decrease of electrode overpotentials upon including an electrolyte–electrode mixture in electrochemical cells to improve the charge transfer process.[31–33] These mixtures are MIEC with lower electronic/ionic ratio than that of the electrode material. Based on this, we believe that $La_2Mo_{2-y}W_yO_{8.96+0.02x}$ could also be tested as interlayers between the electrolyte and the anode expecting to improve the performance of the cells.

As anode materials, they could be used to prepare ceramic/metal composites (CERMETs) by mixing them with a metal like Ni or Cu to obtain an MIEC with higher electronic conductivity. Alternatively, other substitutes to molybdenum could be tested, like mixed-valent metals such as vanadium or chromium, in order to improve the electronic part of conduction in these MIEC materials and make them better anode materials.

Acknowledgements

References

1 P. Lacorre, F. Goutenoire, O. Bohnke, R. Retoux and Y. Laligant, Designing fast oxide-ion conductors based on $La_2Mo_2O_9$, *Nature*, 2000, **404**, 856–858.

2 A. Lashtabeg and S. J. Skinner, Solid oxide fuel cells-a challenge for materials chemists?, *J. Mater. Chem.*, 2006, **16**, 3161.

3 L. Malavasi, H. Kim, S. J. L. Billinge, T. Proffen, C. Tealdi and G. Flor, Nature of the monoclinic to cubic phase transition in the fast oxygen ion conductor $La_2Mo_2O_9$ (LAMOX), *J. Am. Chem. Soc.*, 2007, **129**, 6903–6907.

4 C. Tealdi, G. Chiodelli, L. Malavasi and G. Flor, Effect of alkaline-doping on the properties of $La_2Mo_2O_9$ fast oxygen ion conductor, *J. Mater. Chem.*, 2004, **14**, 3553–3557.

5 X. Wang, Z. Cheng and Q. Fang, Influence of potassium doping on the oxygen-ion diffusion and ionic conduction in the $La_2Mo_2O_9$ oxide-ion conductors, *Solid State Ionics*, 2005, **176**, 761–765.

6 D. Marrero-López, D. Pérez-Coll, J. C. Ruiz-Morales, J. Canales-Vázquez, M. Martin-Sedeño and P. Núñez, Synthesis and transport properties in $La_{2-x}A_xMo_2O_{9-\delta}$ (A = Ca^{2+}, Sr^{2+}, Ba^{2+}, K^+) series, *Electrochim. Acta*, 2007, **52**, 5219–5231.

7 X. P. Wang, Q. F. Fang, Z. S. Li, G. G. Zhang and Z. G. Yi, Dielectric relaxation studies of Bi-doping effects on the oxygen-ion diffusion in $La_{2-x}Bi_xMo_2O_9$ oxide-ion conductors, *Appl. Phys. Lett.*, 2002, **81**, 3434–3436.

8 A. Subramania, T. Saradha and S. Muzhumathi, Synthesis, sinterability and ionic conductivity of nanocrystalline Pr-doped $La_2Mo_2O_9$ fast oxide-ion conductors, *Mater. Chem. Phys.*, 2007, **167**, 319–324.

9 S. Georges, F. Goutenoire, F. Altorfer, D. Sheptyakov, F. Fauth, E. Suard, *et al.*, Thermal, structural and transport properties of the fast oxide-ion conductors $La_{2-x}R_xMo_2O_9$ (R = Nd, Gd, Y), *Solid State Ionics*, 2003, **161**, 231–241.

10 D. Marrero-López, J. Canales-Vázquez, W. Zhou, J. T. S. Irvine and P. Núñez, Structural studies on W^{6+} and Nd^{3+} substituted $La_2Mo_2O_9$ materials, *J. Solid State Chem.*, 2006, **179**, 278–288.

11 G. Corbel, P. Durand and P. Lacorre, Comprehensive survey of Nd^{3+} substitution In $La_2Mo_2O_9$ oxide-ion conductor, *J. Solid State Chem.*, 2009, **182**, 1009–1016.

12 D. Marrero-López, P. Núñez, M. Abril, V. Lavín, U. R. Rodríguez-Mendoza and V. D. Rodríguez, Synthesis, electrical properties, and optical characterization of Eu3+-doped $La_2Mo_2O_9$ nanocrystalline phosphors, *J. Non-Cryst. Solids*, 2004, **345–346**, 377–381.

13 G. Corbel, E. Chevereau, S. Kodjikian and P. Lacorre, Topological metastability and oxide ionic conduction in $La_{2-x}Eu_xMo_2O_9$, *Inorg. Chem.*, 2007, **46**, 6395–6404.

14 S. Basu, P. S. Devi and H. S. Maiti, Nb-Doped $La_2Mo_2O_9$: A New Material with High Ionic Conductivity, *J. Electrochem. Soc.*, 2005, **152**, 2143–2147.

15 Z. S. Khadasheva, N. U. Venskovskii, M. G. Safronenko, A. V. Mosunov, E. D. Politova and S. Y. Stefanovich, Synthesis and Properties of $La_2(Mo_{1-x}M_x)_2O_9$ (M = Nb, Ta) Ionic Conductors, *Inorg. Mater.*, 2002, **38**, 1168–1171.

16 G. Corbel, Y. Laligant, F. Goutenoire, E. Suard and P. Lacorre, Effects of Partial Substitution of Mo^{6+} by Cr^{6+} and W^{6+} on the Crystal Structure of the Fast Oxide-Ion Conductor Structural Effects of W^{6+}, *Chem. Mater.*, 2005, **17**, 4678–4684.

17 J. A. Collado, M. A. G. Aranda, A. Cabeza, P. Olivera-Pastor and S. Bruque, Synthesis, Structures, and Thermal Expansion of the $La_2Mo_{2-x}W_xO_9$ Series, *J. Solid State Chem.*, 2002, **167**, 80–85.

18 S. Georges, F. Goutenoire, Y. Laligant and P. Lacorre, Reducibility of fast oxide-ion conductors $La_{2-x}R_xMo_{2-y}W_yO_9$ (R = Nd, Gd), *J. Mater. Chem.*, 2003, **13**, 2317.

19 D. Marrero-López, J. Canales-Vázquez, J. Ruiz-Morales, J. Irvine and P. Nuñez, Electrical conductivity and redox stability of $La_2Mo_{2-x}W_xO_9$ materials, *Electrochim. Acta*, 2005, **50**, 4385–4395.

20 F. Goutenoire, R. Retoux, E. Suard and P. Lacorre, Ab Initio Determination of the Novel Perovskite-Related Structure of $La_7Mo_7O_{30}$ from Powder Diffraction, *J. Solid State Chem.*, 1999, **142**, 228–235.

21 J. Vega-Castillo, L. Mogni, G. Corbel, P. Lacorre and A. Caneiro, On the thermodynamic stability of $La_2Mo_2O_{9-\delta}$ oxide-ion conductor, *Int. J. Hydrogen Energy*, 2010, **35**, 5890–5894.

22 J. E. Vega-Castillo, U. K. Ravella, G. Corbel, P. Lacorre and A. Caneiro, Thermodynamic stability, structural and electrical characterization of mixed ionic and electronic conductor $La_2Mo_2O_{8.96}$, *Dalton Trans.*, 2012, **41**, 7266–7271.

23 U. K. Ravella, PhD thesis, Université du Maine, Le Mans, 2012.

24 A. Caneiro, Adaptation of an electrochemical system for measurement and regulation of oxygen partial pressure to a symmetrical thermogravimetric analysis system developed using a Cahn 1000 electrobalance, *Rev. Sci. Instrum.*, 1982, **53**, 1072.

25 J. Rodríguez-Carvajal, Recent advances in magnetic structure determination by neutron powder diffraction, *Phys. B: Condens. Matter*, 1993, **192**, 55–69.

26 Scribner Associates, *ZViewTM, A Software Program for IES Measurements and Analysis*, 2007.

27 D. Marrero-López, J. Peña-Martínez, J. Ruiz-Morales, D. Pérez-Coll, M. Martín-Sedeño and P. Núñez, Applicability of $La_2Mo_{2-y}W_yO_9$ materials as solid electrolyte for SOFCs, *Solid State Ionics*, 2007, **178**, 1366–1378.

28 P. Pinet, J. Fouletier and S. Georges, Conductivity of reduced $La_2Mo_2O_9$ based oxides: The effect of tungsten substitution, *Mater. Res. Bull.*, 2007, **42**, 935–942.

29 J. Jacquens, D. Farrusseng, S. Georges, J.-P. Viricelle, C. Gaudillère, G. Corbel, *et al.*, Tests for the Use of $La_2Mo_2O_9$-based Oxides as Multipurpose SOFC Core Materials, *Fuel Cells*, 2010, **10**, 433–439.

30 M. Goel, E. Djurado and S. Georges, Reducibility of $La_2Mo_2O_9$ based ceramics versus porosity, *Solid State Ionics*, 2011, **204–205**, 97–103.

31 T. L. Reitz and H. Xiao, Characterization of electrolyte–electrode interlayers in thin film solid oxide fuel cells, *J. Power Sources*, 2006, **161**, 437–443.

32 F. Zhao and a Virkar, Dependence of polarization in anode-supported solid oxide fuel cells on various cell parameters, *J. Power Sources*, 2005, **141**, 79–95.

33 J. Kim, G. Kim, J. Moon and Y. Park, Characterization of LSM–YSZ composite electrode by ac impedance spectroscopy, *Solid State Ionics*, 2001, **143**, 379–389.